Generalized Parton Distributions and Deep Exclusive Reactions: Present Program at JLab

Michel Garçon

DAPNIA/SPhN, CEA-Saclay, 91191 Gif-sur-Yvette, France

Abstract. We review briefly the physical concept of generalized parton distributions and the experimental challenges associated with the corresponding measurements of deep exclusive reactions. The first data obtained at Jefferson Lab for exclusive photon (DVCS) and vector meson (DVMP) electroproduction above the resonance-excitation region are described. Two upcoming dedicated DVCS experiments are presented in some detail.

GENERALIZED PARTON DISTRIBUTIONS

The physical concepts and underlying theory of generalized parton distributions (GPD) were to be reviewed at this Workshop by A. Schäfer, who could not attend. We certainly missed his insight and rigor on the subject. In a much more heuristic way than he would have done, I recall some of the main features of GPDs.

In the Bjorken limit, exclusive processes of the type $\gamma^* p \to p\gamma, \pi, \rho, \omega \cdots$ are described in term of a handbag diagram. The corresponding amplitude factorizes [1, 2] into a hard scattering process involving one participant parton (e.g. $\gamma^* q \to \gamma q$) and a soft rearrangement in the nucleon parameterized by four GPDs, denoted by H, E ("unpolarized" or more exactly independent of the quark helicity) and $\tilde{H}, \tilde{E}$ ("polarized"). In addition to the scale variable Q^2, these are functions of three variables: x, the average longitudinal parton momentum fraction before and after the hard scattering; ξ, half the difference between these two momentum fractions, and a four-momentum transfer squared t.

An oversimplified physical image can be given in terms of ordinary quantum mechanics. Schematically, a nucleon reduced to a 3-quark configuration can be described by a wave function $\psi(x_1, \vec{k}_1, x_2, \vec{k}_2, x_3, \vec{k}_3)$ where x is again a parton longitudinal momentum fraction and $\vec{k}$ its transverse momentum. An "ordinary" parton distribution is given by the probability integral

$$q(x) \sim \int |\psi(x, \vec{k}_1, x_2, \vec{k}_2, x_3, \vec{k}_3)|^2 [dX] \tag{1}$$

with $[dX] = \delta(x+x_2+x_3-1)\delta^{(2)}(\vec{k}_1+\vec{k}_2+\vec{k}_3)dx_2dx_3d\vec{k}_1d\vec{k}_2d\vec{k}_3$. In this representation, a GPD can be thought of as an overlap integral

$$H(x,\xi,t) \sim \int \psi^*(x-\xi,\vec{k}_1+\vec{\Delta}_\perp,x_2,\vec{k}_2,x_3,\vec{k}_3)\cdot\psi(x+\xi,\vec{k}_1,x_2,\vec{k}_2,x_3,\vec{k}_3)[dX] \qquad (2)$$

The off-diagonal character of the GPD appears in the change of longitudinal momentum: a GPD thus expresses the *coherence* between states of different longitudinal momenta. Kinematically, this rearrangement cannot occur without a non-zero squared momentum transfer $t = f(\xi,\vec{\Delta}_\perp)$. Through a Fourier transform with respect to $\vec{\Delta}_\perp$ at $\xi = 0$, GPDs can be related to spatial transverse distributions of partons. Thus, through the *x*-*t* correlation, the GPDs contain information about the transverse distribution of partons of given *x*. This opens the way for a femto-photography of the nucleon. Qualitatively, this correlation between the transverse position $\vec{b}$ and the longitudinal momentum $\vec{p}$ gives also access to information about the orbital angular momentum of the partons ($\vec{b}\wedge\vec{p}$).

This picture can be extended to include quark-antiquark configurations in the initial and/or final states.

EXPERIMENTAL CHALLENGES

At high virtuality Q^2 of the exchanged photon, the measurements of exclusive production reactions are very challenging. Precision measurements require high luminosity $\times$ acceptance since the cross sections are small. Exclusivity is necessary for a quantitative comparison with theory and for a detailed study of scaling laws. This puts high demands on resolution and/or complete coverage of reaction products. For example, in the $ep \to ep\gamma$ process, it is in principle sufficient to identify two of the three particles in the final state and measure their momentum vector (this is the case in the first two graphs of figure 1). In practice, as beam and secondary particles energies increase, it becomes increasingly difficult to separate DVCS from exclusive π^0 production when measuring only the scattered electron and proton (third graph of fig. 1). It is then necessary to detect all three particles in the final state.

DEEPLY VIRTUAL COMPTON SCATTERING

The first measurements of beam spin asymmetry in the $\vec{e}p \to ep\gamma$ exhibit an azimuthal dependence characteristic of the interference of a helicity conserving process such as DVCS with the Bethe-Heitler process [4, 5]. Moreover the magnitude of this asymmetry is agreement with models based on GPDs, including small higher-twist contributions and next-to-leading order α_S corrections. Note however that the same results may also be described within a Regge model [6].

Since then, other CLAS data taken at beam energies of 4.8 and 5.75 GeV are being analyzed as well. This is still based on the study of $ep \to epX$ configurations. At 4.8 GeV, the resolution still allows to perform a shape analysis of the missing mass spectra, similar to the procedure in Ref. [4], thus separating the γ and π^0 contributions [7]. An

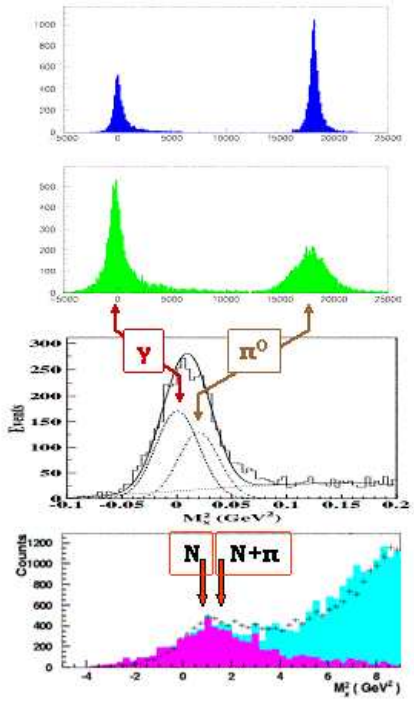

FIGURE 1. Squared missing mass for performed VCS or DVCS experiments. From top to bottom: $ep \to epX$ from MAMI (850 MeV beam energy) [3], from JLab/Hall A (4 GeV) [3], and from JLab/CLAS (4.2 GeV) [4], $ep \to e\gamma X$ from HERMES (27 GeV) [5].

exemple of such a separation is given in the third graph of fig. 1, where each contribution is independently calibrated using subsets of unambiguously identified events [4]. At 5.75 GeV, the missing mass resolution worsens and precludes such an analysis. The pion contribution is then minimized (but not yet quantified) through an approriate choice of kinematical cuts, guided by a Monte-Carlo simulation of both processes [8]. In both cases, earlier results are confirmed, and the higher statistics allow for a finer binning, in Q^2, x_B and/or t. The measured beam spin asymmetry, at fixed x_B and t, is consistent with a $1/Q$ behaviour, as expected from the leading-twist (handbag) contribution to DVCS.

Target spin asymmetries, using a polarized NH_3 target, were investigated as well [9]. Here again the contribution of the $ep \to ep\pi^0$ process remains to be quantified.

Dedicated experiments now aim at detecting the three particles in the final state, in order to ensure a complete exclusivity in the measurements. See figure 2.

In CLAS [10], the photons emitted in a forward cone (3-14°) will be detected in a new inner calorimeter, consisting of 424 small lead-tungstate crystals read by avalanche photodiodes. In addition, a specifically designed two-coil solenoid will focus the background low energy electrons along the beam axis. A 100-crystal prototype was tested with success in December 2003. The whole experiment is to be mounted in February

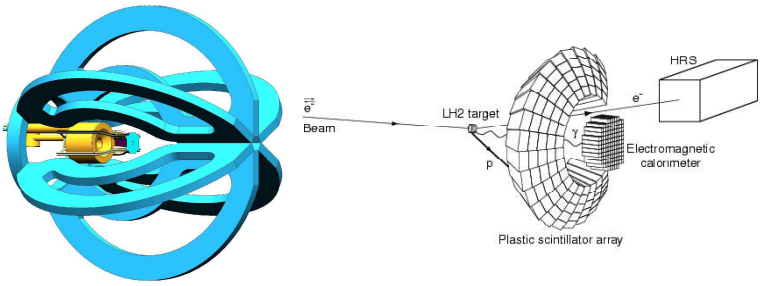

FIGURE 2. Shematic views of dedicated CLAS (left) and Hall A (right) DVCS experiments. The standard CLAS detection is not shown; the new solenoid and calorimeter are positioned at the center of the CLAS toroidal magnet.

2005.

In Hall A [11], a lead-fluoride calorimeter is mounted in direct view of the target, along the direction of the virtual photon, for each of three spectrometer settings for the scattered electron. The recoil protons are detected in a concentric annular plastic scintillator array. The experiment is currently running at the designed luminosity of 10^{37} cm^{-2}s^{-1}. A follow-up experiment will study DVCS on the neutron [12]. The quasi-free $e(n) \rightarrow en\gamma$ reaction will be measured using a liquid deuterium target and complementing the proton array with thin scintillator for proton/neutron discrimination. The DVCS beam spin asymmetry on the neutron has been shown to be more sensitive to the quark total angular momentum in the nucleon.

Double DVCS ($ep \rightarrow epe^+e^-$ proceeding through $\gamma^* q \rightarrow \gamma^* q$) has the potential to access GPDs at a tunable kinematical point $x = f(\xi, q'^2)$, where q'^2 is the virtuality of the outgoing photon (or equivalently the invariant mass of the corresponding lepton pair) [17]. Positrons were cleanly selected in CLAS and $ep \rightarrow epe^+X$ configurations analyzed [18]. Although $ep \rightarrow epe^+e^-$ events could be clearly identified, the analysis faces a theoretical and experimental challenge: there are two electrons in the final state. Antisymmetrisation was not taken into account in the calculations. Experimentally, the kinematical variables depend on the identification of an electron either as scattered or coming from the lepton pair. One of the two possible choices result in the observation of clear peaks associated with very low Q^2 vector meson production. Our preliminary conclusion is then that the observed $ep \rightarrow epe^+e^-$ events cannot be interpreted in the framework of DDVCS and GPDs.

DEEPLY VIRTUAL MESON PRODUCTION

The hard electroproduction of mesons, or DVMP, should also proceed through the same handbag diagram. In this case, factorization has been demonstrated for longitudinal virtual photons [2]. According to the nature of the emitted meson, one probes different GPDs (H and E for vector mesons, $\tilde{H}$ and $\tilde{E}$ for pseudoscalar mesons) and different flavor combinations (e.g. ρ vs ω, or π^0 vs η). The difficulty here is in isolating the contribution of longitudinal photons and reaching high enough Q^2, since the additional gluon exchange necessary to produce the meson moves the asymptotic regime to higher values of Q^2.

Longitudinal cross sections have been extracted for ρ electroproduction at 4.2 GeV [13]. A similar analysis for higher energy (5.75 GeV), with higher statistics data, is underway. In this channel, both the CLAS and HERMES data are in semi-quantitative agreement with a model based on GPDs, and including an effective description of higher-twist effects.

The ϕ [14] and ω [15] channels have been analyzed as well. In the latter case, a determination of the emitted ω spin density parameters led to the conclusion that helicity is not conserved between the virtual photon and the emitted meson. Thus the handbag diagram does not dominate the reaction $ep \rightarrow ep\omega$ and the longitudinal cross sections could not be extracted. The ω channel thus appears the most challenging one to access the GPDs. Within a Regge approach, it was shown that this behaviour is due to the dominantly transverse t-channel π^0 exchange, or rather the exchange of the corresponding saturating Regge trajectory [16]. Only for the ω channel is this specific exchange contribution dominant. This calculation gives a new insight in the high-Q^2 and high-t behaviour of such exclusive reactions [16].

CONCLUSIONS

Generalized Parton Distributions have merged as a powerful, attractive and unifying concept for the nucleon structure. The relation between GPDs and deep exclusive reactions still needs experimental validation. There are experimental indications that the handbag diagram is at work in DVCS and this is being studied with increased statistics data sets at CLAS. In DVMP, extensive data sets on vector meson production, also from CLAS, will be coming shortly. Dedicated DVCS experiments, in Hall A (2004) and CLAS (2005), will measure beam spin asymmetries, detecting all three particles in the final state to ensure full exclusivity. They should establish on firm grounds the validity of the approach. Detailed tests of scaling will be performed. If scaling is indeed observed, or deviations thereof understood, these experiments, in conjunction with theoretical input, will provide the first significant measurements of GPDs.

REFERENCES

1. X. Ji, Phys. Rev. D **55** (1997) 7114; A.V. Radyushkin, Phys. Rev. D **56** (1997) 5524.
2. J.C. Collins, L. Frankfurt, and M. Strikman, Phys. Rev. D **56** (1997) 2982-3006.

3. H. Fonvieille, private communication.
4. S. Stepanyan *et al.* (CLAS collaboration), Phys. Rev. Lett. **87** (2001) 182002.
5. A. Airapetian *et al.* (HERMES collaboration), Phys. Rev. Lett. **87** (2001) 182001.
6. F. Cano and J.-M. Laget, Phys. Lett. **B**551 (2003) 317.
7. G. Gavalian *et al.* (CLAS collaboration), preliminary results.
8. H. Avakian *et al.* (CLAS collaboration), preliminary results.
9. S. Cheng *et al.* (CLAS collaboration), preliminary results.
10. V. Burkert, L. Elouadrhiri, M. Garçon, S. Stepanyan *et al.*, CEBAF experiment 01-113.
11. P. Bertin, C. Hyde-Wright, R. Ransome, F. Sabatié *et al.*, CEBAF experiment 00-110.
12. P. Bertin, C. Hyde-Wright, F. Sabatié, E. Voutier *et al.*, CEBAF experiment 03-106.
13. C. Hadjidakis *et al.* (CLAS collaboration), hep-ex/0408005.
14. J. Santoro *et al.* (CLAS collaboration), preliminary results.
15. L. Morand *et al.* (CLAS collaboration), in preparation. M. Garçon, contr. to the *10th Int. Symp. on Meson-Nucleon Physics and the Nucleon Structure*, Beijing, Aug. 2004.
16. J.-M. Laget, Phys. Rev. D **70** (2004) 054023.
17. M. Guidal and M. Vanderhaeghen, Phys. Rev. Lett. **90** (2003) 012001; A.V. Belitsky and D. Müller, Phys. Rev. Lett. **90** (2003) 022001.
18. S. Morrow, M. Garçon *et al.* (CLAS collaboration), preliminary results.